**Korean Chem. Eng. Res.,** 63(2), 105107 (2025)
https://doi.org/10.9713/kcer.2025.63.2.105107
PISSN 0304-128X, EISSN 2233-9558

# Multi-Objective Optimization for Improved Energy and Exergy Efficiency and Total Cost Reduction in Cascade Refrigeration Systems

**Mostafa Dehghani*,**,† and Mohsen Mozafari_Shamsi***

**Department of Engineering, Meybod university, Yazd, Iran*
***Department of Mechanical Engineering, University of Sistan and Baluchestan, Zahedan, Iran*
(Received 25 November 2024; Received in revised from 13 February 2025; Accepted 24 February 2025)

**Abstract** – In this article, a three-objective optimization technique constructed on Non-dominated Sorting Genetic Algorithm (NSGA-II) was used to increase the coefficient of performance (COP) and exergy efficiency (η) of a two-stage vapor compression cascade refrigeration system (CCRS) and decrease its total cost rate ($\dot{C}_t$). The model was built in MATLAB and the refrigerants thermo-physical properties were probed by using REFPROP. Since refrigerant mixtures with zeotropic behavior can improve the energy efficiency of the system, the binary refrigerant mixtures with variable mass fractions were used on both sides of CCRS. The cycle optimization was done based on 10 design variables. The first six design variables were refrigerant type and their mass fractions on the low temperature cycle (LTC) and high temperature cycle (HTC). The saturated vapor temperature in the condenser and cascade heat exchanger (CHX) inlets, the evaporator inlet temperature, and the two-phase temperature in the CHX inlet were selected as the remaining four design variables. The cooling capacity and evaporator and condenser secondary flow conditions were kept fixed during the optimization process. The comparison of optimization results with the base case showed a 15.55% and 17.74% increase in COP and η, respectively. while the total cost rate ($\dot{C}_t$) showed a 6.07% reduction. Finally, the optimization process led to a 24.47% and 13.1% reduction in the CCRS cycle total exergy destruction and maximum cycle temperature.

Key words: Cascade refrigeration, Coefficient of performance, Exergy efficiency, Cost analysis, Three-objective optimization, Mixed refrigerant

## 1. Introduction

Refrigeration is a crucial technology that plays a vital role in various sectors, including food preservation, pharmaceuticals, and industrial processes. It involves the removal of heat from a designated area to lower its temperature, thereby maintaining the quality and safety of perishable goods and enhancing the performance of numerous applications. As global demand for energy-efficient cooling solutions continues to grow, there is an increasing emphasis on improving energy efficiency to reduce operational costs and carbon footprints in both residential and industrial settings. Cascade refrigeration systems (CRS) have emerged as a promising solution to meet these challenges. These systems employ two or more refrigeration cycles arranged in series, allowing for effective cooling across a wide temperature range. By utilizing different refrigerants optimized for specific temperature domains, cascade systems enhance efficiency and performance, making them ideal for applications such as cryogenics, high-temperature superconductors, and industrial cooling processes. Furthermore, as industries strive to comply with stringent regulations regarding refrigerant use and energy consumption, the development of advanced cascade systems stands at the forefront of engineering efforts to create sustainable cooling solutions.

The two-stage CCRS is a kind of cascade refrigeration system including two cycles, LTC and HTC. The cycles are coupled by a heat exchanger. This heat exchanger which sometimes called cascade condenser, is employed as the evaporator of LTC and condenser of HTC [1,2]. the performance analysis of a two stage CRS working with dimethyl ether as HTC fluid and the mixtures of carbon dioxide and hydrocarbons (propane, ethane, ethylene, and propylene) as LTC fluid was studied by Di Nicola et al. [3]. Results showed that by mixing R744 to HCs the COP of cycle and mixture flammability decreased. A two-stage CRS using the binary mixtures of R744/R717, R744/R1270, and R744/RE170 was studied by Massuchetto et al. [4]. The mass fraction of refrigerants in the mixtures plus LTC condensation temperature were selected as inputs for parametric study. While, compressor work, refrigerant mass flow rate in LTC and HTC cycles, exergy destruction rate, exergy efficiency, and COP were used as outputs. By fixing the cooling capacity on 100 kW and using the Aspen Hysys® software the systems were optimized to maximize the COP. After all, the mixture of R744/RE170 resulted a maximum COP of 2.34 (32% increase in COP comparing to the pure refrigerants). Various zeotropic blends composed of $CO_2$ compared theoretically and experimentally with pure $CO_2$ in a single-stage vapor compression cycle equipped with an internal heat exchanger by Sánchez et al. [5]. The analysis suggested replacement of pure $CO_2$ with mixtures of

† To whom correspondence should be addressed.
E-mail: m_dehghani@meybod.ac.ir, m_dehghani@eng.usb.ac.ir

$CO_2$/R1270 and $CO_2$/R32 to reduce energy and power consumptions. In conclusion, using $CO_2$ mixture demonstrated the capability of efficiently enhancing the $CO_2$ transcritical cycle's performance without using the complex arrangements mainly used in high-capacity systems.

Energy systems optimization (especially cascade refrigeration cycle optimization) is very important and many researchers paid attention to this topic. Sun et al. [6] studied a comparative analysis of the thermodynamic performance of a CRS for refrigerant pairs R23/R404A and R41/R404A. In their research the evaporating and condensing temperatures, and subcooling and superheating temperatures were selected as decision variables. Also, the power consumption of compressor and its discharge temperature, COP, exergy loss (X), and exergy efficiency (η) were selected as objective functions. The analysis indicated that there was an optimum condensing temperature for LTC that resulted in maximum COP. In addition, their results indicated the superior performance of R41/R404A refrigerant pair in the CRS. The multi-objectives optimization of a CRS using a mixture of $C_2H_6/CO_2$ in LTC and $C_3H_8$ in HTC was performed by Nasruddin et al. [7]. In this study, the condenser and evaporator temperatures, LTC condensation temperature, cascade temperature differences, and mass fraction of $CO_2$ were chosen as the decision variables. Also, the total exergy destruction and total annual cost were used as objective functions. Results showed that, by trade-off between the two objective functions the optimum value of the decision variables can be calculated. By using a heat transfer search algorithm Patel et al. [8] performed the optimization of a CRS using $NH_3/CO_2$ and $C_3H_8/CO_2$ mixtures to minimize the total annual cost and exergy destruction of the cycle. The evaporator and condenser temperatures, the condenser temperature of LTC, and cascade temperature difference were selected as design variables. Results revealed that the $C_3H_8/CO_2$ mixture can offer 5.33% lower cost and 6.42% higher exergy destruction compared to the $NH_3/CO_2$ mixture. The multi-objective optimization of CRS equipped with heat recovery system has been investigated by Golbaten Mofrad et al. [9]. The R744 and R744A refrigerants were used for the HTC and LTC, respectively. The COP, exergy efficiency, total product cost and product environmental impact were selected as objective functions. Results revealed that the use of heat recovery in CRS can increase the COP and exergy efficiency about 7.6% and 12.5%, respectively. By using the concept of modified and advanced exergy, risk level, and thermal inventory Jain et al. [10] performed a multi-objective optimization of CRS. Their results showed a 10.2% and 8.9% decrease in total irreversibility and annual risk level and a 6.8% increase in thermal inventory, respectively. Zhu et al. [11] studied an innovative multi-target-temperature cascade (MTTC) refrigeration cycle. The cycle used R717 in the HTC and R744 and R1270 individually in the LTC. The results showed a better thermodynamic performance for the MTTC system at low temperatures. Yoon et al. [12] used Aspen HYSYS V12 for energy and exergy analysis of a cascade mixed refrigerant joule–Thomson system with a precooler. Researchers used a combination of R23, R218, R14, and Ar. Results showed a 21.6%, and 47.4% increase in COP and exergy efficiency of the system, respectively. Ghosh et al. [13] performed a theoretical analysis of the r1234yf/$co_2$ cascade refrigeration system by using energy equation software (EES). The researchers obtained optimum results for COP, exergy efficiency, and total exergy destructions. Liu et al. [14] delved into the realm of energy and exergy analysis, to optimize the COP of refrigeration cycle. The analysis was conducted within the EES software environment. Their results showed a 21%, and 32% increase in COP and exergy efficiency. In addition, Liu et al. [15] designed an experimental setup to evaluate an ultra-low cascade freezer performance by using R290 and R170 refrigerants. The results showed that by increasing the ambient temperature from 16℃ to 32℃, the energy demand of the CRS increased from 896W to 912W. While, lowering freezer temperature from −60℃ to −86℃ led to increase increase in power consumption from 804W to 904W. Finally, the multi-objective optimization of an ultra-low temperature CRS using response surface methodology and desirability approach was presented by Ye et al. [16]. The design variables were selected as evaporation temperature, HTC and LTC condensing temperatures, temperature difference in cascade heat exchanger, and refrigerant superheat at compressor inlet. While, the COP, total exergy destruction, and exergy efficiency were chosen as objective functions. The results showed a very good agreement between the predicted and actual values for the COP and exergy efficiency.

As mentioned above, a brief review of the literature showed that some researchers used only single refrigerant for the low temperature cycle (LTC) and high temperature cycle (HTC) of cascade refrigeration cycle [2,6,8,9,11,13-17]. While some other used a single refrigerant for one of the cycles and a mixed refrigerant for other cycle [3,7]. Additionally, there were some works that used mixed refrigerants for LTC and HTC, simultaneously [4,5,12]. It may be because the mentioned manuscripts were devoted to simple refrigeration cycle, or Joule–Thomson System, or optimized some aspects such as energy efficiency, exergy efficiency, and cost analysis. So, the goal of current work is to optimize the energy efficiency, exergy efficiency and total annual cost of a CRS by using the mixed refrigerants on the both sides of the cascade cycle. Additionally, the effect of each component on total exergy destruction for the base and optimized cases are studied and compared. Furthermore, the distinction of the current research with the prior techniques, including the methods, application, selected refrigerants, and analysis type is presented in Table 1.

## 2. Problem Statement and Governing Equations

### 2-1. Cycle description

A schematic of the CRS used for energy and exergy analysis was shown in Figure 1. Figure 1, showed the simple two-stage vapor compression refrigeration system (VCRS), which was composed of two independent compression cycles (LTC, HTC) connected by a cascade condenser. In this cycle, the evaporated refrigerant (point 1)

**Table 1. A brief summary of the investigations in the field of cascade refrigeration**

| Author | Method | Application | | | Refrigerant Types | | | | Analysis | | |
|---|---|---|---|---|---|---|---|---|---|---|---|
| | | | | | Single | | Mixed | | | | |
| | | VCRS | CCRS | Other | LTC | HTC | LTC | HTC | Energy | Exergy | Cost |
| Dopazo et al. [2] | Theoretical | | ✓ | | $Co_2$ | $NH_3$ | | | ✓ | ✓ | |
| Sun et al. [6] | Theoretical | | ✓ | | R23<br>R41 | R404A | | | ✓ | ✓ | |
| Patel et al. [8] | Theoretical | | | | $Co_2$ | $NH_3$<br>$C_3H_8$ | | | | ✓ | ✓ |
| Golbaten Mofrad et al. [9] | Theoretical | | ✓ | | R744A | R744 | | | ✓ | ✓ | ✓ |
| Zhu et al. [11] | Theoretical | | ✓ | | R744<br>R1270 | R717 | | | ✓ | ✓ | ✓ |
| Ghosh et al. [13] | Theoretical | | ✓ | | $Co_2$ | R1234yf | | | ✓ | ✓ | |
| Liu et al. [15] | Experimental | | ✓ | | R290 | R170 | | | ✓ | | |
| Liu et al. [14] | Theoretical | | ✓ | | R407C<br>R290<br>R134a<br>R500 | | | | ✓ | ✓ | |
| Ye et al. [16] | Theoretical | | ✓ | | R170 | R290 | | | ✓ | ✓ | |
| Rezayan and Behbahaninia [17] | Theoretical | | ✓ | | $Co_2$ | $NH_3$ | | | ✓ | ✓ | ✓ |
| Di Nicola et al. [3] | Theoretical | | ✓ | | | Dimethyl ether | $Co_2$ based blends | | ✓ | | |
| Nasruddin et al. [7] | Theoretical | | ✓ | | | $C_3H_8$ | mixture of $C_2H_6/Co_2$ | | | ✓ | ✓ |
| Massuchetto et al. [4] | Theoretical | | ✓ | | | | R744/R1270<br>R744/R717<br>R744/RE170 | | ✓ | ✓ | |
| S´anchez et al. [5] | Experimental/ Theoretical | ✓ | | | | | $Co_2$ binary blends | | ✓ | | |
| Yoon et al. [12] | Theoretical | | | ✓ | | | mixture of R218, R23, R14, and Ar | | ✓ | ✓ | |

was transferred to the low-stage compressor and after compression, superheated vapor (point 2) entered the cascade condenser. Inside the CHX (usually shell and tube type) the superheated vapor in LTC transferred its heat to the HTC refrigerant and after condensation left at point 3, while the two-phase refrigerant flowing in the HTC (point 8) due to heat transfer changed its phase and left the cascade heat exchanger as a saturated or superheat vapor (point 5). Then, the condensed refrigerant in the LTC (point 3) passed through the expansion device and moved into the evaporator as a two-phase mixture (point 4). The refrigerant vapor leaving the cascade heat exchanger (point 5) moved to high-temperature compressor and left it at high temperature and pressure (i.e., superheat). The superheated refrigerant at HTC (point 6) moved into the condenser and transferred its heat to the condenser cooling medium and left the condenser as a liquid or subcooled liquid (point 7). Finally, the condensed liquid passed through the expansion valve (throttling process) and after pressure and temperature reduction entered the evaporator (point 8).

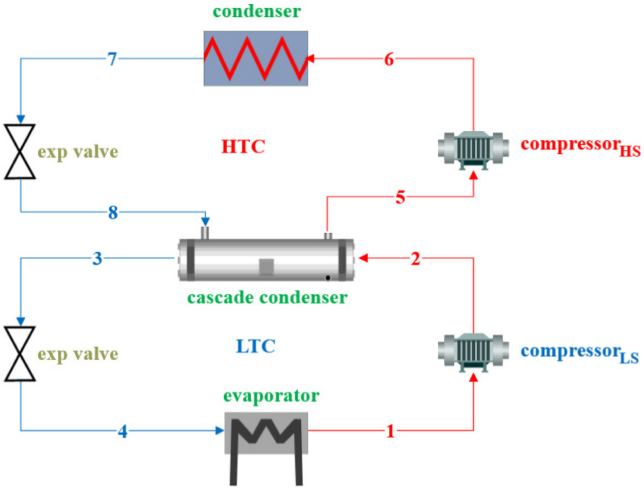


**Fig. 1. The two-stage VCRS.**

### 2-2. Governing equations and assumptions

The assumptions for the simulation of CCRS were steady-state conditions, neglecting pressure drop in heat exchangers and connecting pipes, and negligible kinetic and potential energy change in all system components. Also, there was no heat transfer between components and surroundings (i.e., the heat loss to surroundings is negligible). In regard to the Heggs [18] and Oh et al. [19] suggestions, the minimum temperature approach of CHX was fixed at 5℃. Refrigerants leaving condensers (e.g., points 3 and 7 in Fig. 1)) were assumed saturated liquid. Similarly, refrigerants leaving evaporators (e.g., points 1 and 5 in Fig. 1) were assumed saturated vapor. The expansion process in the throttling valves was assumed isenthalpic. Based on Oh et al. [19] recommendations, the isentropic efficiency for LTC and HTC compressors was fixed at 80%. Also, the combined electromotor and

1mechanical efficiency of compressors was supposed to be 100%.

For proposed mixed refrigerants with zeotropic behavior, there was a temperature glide and the temperature during phase change was not constant. So, to compare the performance of different refrigeration cycles a suitable reference temperature must be used as proposed by McLinden and Radermacher [20]. Here, the selected constant temperatures were saturated vapor temperature in the condenser ($T_{6,sv}$) in Fig. 1) and evaporator inlet temperature (e.g., ($T_4$) in Fig. 1). The mass balance for steady-state operation was as follows,

$$\sum_{in}\dot{m} = \sum_{out}\dot{m} \tag{1}$$

Steady-state energy relation for each control volume can be written as follows:

$$\dot{Q}_{in} - \dot{W}_{in} = \sum_{out}\dot{m}\left(h + \frac{V^2}{2} + gz\right) - \sum_{in}\dot{m}\left(h + \frac{V^2}{2} + gz\right) \tag{2}$$

In heat exchangers, temperature glides were calculated as below:

$$\Delta T_{glide}(^{\circ}\mathrm{C}) = T_{sv} - T_{sl} \tag{3}$$

The COP of CCRS can be defined as:

$$\mathrm{COP} = \frac{\dot{Q}_{evp}}{\dot{W}_t} \tag{4}$$

Where total work was the sum of work required by LTC and HTC compressors ($\dot{W}_t = \dot{W}_{LTC} + \dot{W}_{HTC}$). While the cooling capacity of the cycle ($\dot{Q}_{evp}$) was considered fixed and equal to 100 kW.

Exergy balance equation for any control volume, in the steady-state condition, can be presented as follows:

$$\sum_{j}\left(1 - \frac{T_{Surr,j}}{T_{Hs,j}}\right)\dot{Q}_j - \dot{W} + \sum_{in}\dot{m}\psi - \sum_{out}\dot{m}\psi - \dot{X} = 0 \tag{5}$$

Where $T_{Hs,j}$ was the mean temperature of the heat source in the cold and hot sides of CCRS, and $T_{Surr,j}$ was the temperature of the surrounding. For exergy analysis, the surrounding temperature $T_0$ was equal to 298.15 K. Flow physical exergy at any stage of any system ($\psi$) can be defined as:

$$\psi = (h_{in} - h_{out}) - T_0(s_{in} - s_{out}) \tag{6}$$

The exergy destruction of components in the cycle can be estimated by using equations (5) and (6). Also, the parameter $\delta$ was defined as the portion of the cycle's components in the total exergy destruction:

$$\delta_i = \frac{\dot{X}_i}{\dot{X}_t} \tag{7}$$

Where $\dot{X}_{tot}$ was the total exergy destruction. Finally, the net exergy efficiency of the cycle was defined as:

$$\eta = \frac{\text{Exergy recovered}}{\text{Exergy supplied}} = \frac{\dot{W}_t - \dot{X}_i}{\dot{W}_t} = 1 - \frac{\dot{X}_i}{\dot{W}_t} \tag{8}$$

The details of energy and exergy balance relations for CCRS were given in Table 2.

The capital cost, maintenance cost and operational cost of components must be calculated in the economic analysis. Therefore, the total cost rate of the CRS ($\dot{C}_t$) including the cycle's initial investment and maintenance cost rates ($\sum \dot{Z}_k$) and operational cost rate ($\dot{C}_{op}$) can be expressed as follows [21]:

$$\dot{C}_t = \sum_k \dot{Z}_k + \dot{C}_{op} \tag{9}$$

Based on the cost functions suggested by Rezayan and Behbahaninia [17] the capital cost of each component ($Z_k$) in terms of US dollars has been estimated. It should be noted that the costs related to the expansion valves, as well as the condenser and evaporator fans, were neglected.

$$Z_{comp,HTC} = 9624.2\ \dot{W}_{HTC}^{0.46} \tag{10}$$

$$Z_{comp,LTC} = 10167.5\ \dot{W}_{LTC}^{0.46} \tag{11}$$

$$Z_{cond} = 9624.2\ A_{cond}^{0.89} \tag{12}$$

$$Z_{evp} = 9624.2\ A_{evp}^{0.89} \tag{13}$$

$$Z_{cas,cond} = 92382.9\ A_{cas,cond}^{0.68} \tag{14}$$

Usually, the unit of time interval selected for capital cost analysis was taken as a year. By using the capital recovery factor (CRF) [22], the capital cost in a year was calculated:

$$CRF = \frac{i(1+i)^n}{(1+i)^n - 1} \tag{15}$$

**Table 2. Energy and exergy relations for CCRS (Fig. 1)**

| Component | Simple CCRS | |
|---|---|---|
| | Energy equation | Exergy equation |
| Evaporator | $\dot{Q}_{evp} = \dot{m}_{LTC}(h_1 - h_4)$ | $\dot{X}_{evp} = \dot{m}_{LTC}\left((\psi_4 - \psi_1) + \dot{Q}_{evp}\left(1 - \frac{T_{CL}}{T_{evp}}\right)\right)$ |
| LTC compressor | $\dot{W}_{LTC} = \dot{m}_{LTC}(h_2 - h_1)$ | $\dot{X}_{comp,LTC} = \dot{m}_{LTC}(\psi_1 - \psi_2) + \dot{W}_{LTC}$ |
| CHX | $\dot{m}_{LTC}(h_2 - h_3) = \dot{m}_{HTC}(h_5 - h_8)$ | $\dot{X}_{comp,cond} = \dot{m}_{LTC}(\psi_2 - \psi_3) + \dot{m}_{HTC}(\psi_8 - \psi_5)$ |
| LTC throttle valve | $h_3 = h_4$ | $\dot{X}_{exp,LTC} = \dot{m}_{LTC}(\psi_3 - \psi_4)$ |
| HTC compressor | $\dot{m}_{HTC} = \dot{m}_{HTC}(h_6 - h_5)$ | $\dot{X}_{comp,HTC} = \dot{m}_{HTC}(\psi_5 - \psi_6) + \dot{W}_{HTC}$ |
| Condenser | $\dot{Q}_{cond} = \dot{m}_{HTC}(h_6 - h_7)$ | $\dot{X}_{cond} = \dot{m}_{HTC}\left((\psi_6 - \psi_7) + \dot{Q}_{cond}\left(1 - \frac{T_0}{T_{cond}}\right)\right)$ |
| HTC throttle valve | $h_7 = h_8$ | $\dot{X}_{exp,HTC} = \dot{m}_{HTC}(\psi_7 - \psi_8)$ |

Here, the terms $n$ and $i$ were the system lifetime and the interest rate, respectively. Furthermore, to convert the capital costs (in $) into the cost rate $\dot{Z}_k$ ($/hr), one may write:

$$\dot{Z}_k = \frac{Z_k \times CRF \times \varphi}{N} \tag{16}$$

where $\varphi$ and $N$ were the maintenance factor and the annual operational hours of the system, respectively. The following equation can be used to calculate the operational cost of CRS. The operational cost was related to the power consumption of compressors.

$$\dot{C}_{op} = \dot{W}_t \times C_{el} \tag{17}$$

where $C_{el}$ was the unit cost of electricity and its value depend on the working hours of the cycle.

### 2-3. Multi-objective optimization

The genetic algorithm (GA) was a heuristic method inspired by Darwin's laws of natural selection [23]. In this article to improve the CCRS cycle performance a multi-objective optimization based on the Non-dominated Sorting Genetic Algorithm (NSGA-II) was used. The initial population for the optimization process was selected as 50 and about 150 iteration was used. Also, A crossover and mutation rate of 70% and 30% were used for producing new offsprings during optimization.

The COP was a positive number greater than 1, while the exergy efficiency ($\eta$) was a non-dimensional number between 0 and 1. Both of them must be maximized, while the total cost rate was a positive number greater than 1 and must be minimized. Therefore, the NSGAII was used to maximize the three outputs of the following goal function:

$$[COP, \eta, -\dot{C}_t] = f(R_{LTC,f}, R_{LTC,s}, Mf_{LTC}, R_{HTC,f}, Mf_{HTC}, T_{2,sv}, T_{6,sv}, T_4, T_8) \tag{18}$$

The multi-objective optimization was done based on 10 design variables. The design variables included the refrigerant type, their mass fractions in the LTC and HTC of the cycle, and four temperatures. In this study, two refrigerants (chosen from $CO_2$, DME, and Propylene) and one mass fraction for both the LTC and HTC were used as design variables. Additionally, the saturated vapor temperatures in the condenser and cascade condenser inlets ($T_{6,sv}$, $T_{2,sv}$) as well as the refrigerant temperatures in the evaporator and cascade heat exchanger inlets ($T_4$, $T_8$) were selected as the remaining design variables. The suggested design variables and their corresponding ranges for the multi-objective optimization of the CCRS have been presented in Table 3.

While our approach was robust, there were situations where it might face limitations. For instance, the range of variation for the evaporator inlet temperature must be compatible with the normal boiling point (NBP) and freezing point of the selected refrigerants. Currently, the normal boiling points of R744 ($Co_2$), RE170 (DME), and R1270 (Propylene) were -78.4℃, -24.78℃, and -47.7℃, respectively. The freezing points of these refrigerants were -78.5°C, -57℃, and -185℃, respectively. As a result, the evaporator inlet temperature ($T_4$) was limited to between -21℃ and -40℃, which was significantly above the freezing point of these mixtures. Additionally, the evaporator pressure was certainly above normal atmospheric pressure, allowing for easy diagnosis of any leakage in the equipment and piping system. Also, it should be noted that the mass fraction of the second refrigerant in LTC and HTC can be calculated by subtracting the first refrigerant mass fraction from 1.

## 3. Results and Discussion

To verify the numerical simulation method, the accuracy of the current code was compared with the numerical solutions reported by Massuchetto et al. [4] for a two-stage vapor compression cascade refrigeration cycle (i.e., Fig. 1). The cooling capacity of CCRS was fixed at 100 kW in the evaporator to decrease the temperature of a secondary fluid from -5℃ to -20℃. The optimized operating conditions of studied mixed refrigerant suggested by Massuchetto et al. [4] were used to compare COP, exergy efficiency, and operating conditions. The results were presented in Table 4. Additionally, the T-s diagram of the cycle (for $CO_2$/Propylene pairs) was illustrated in Fig. 2. As shown in this figure, during the phase change, the temperature of the binary mixture varied, resulting in a temperature glide for both LTC and HTC.

As shown in Table 4, the relative errors between the current numerical code and numerical solutions presented by [4] were in good agreement. Additionally, the numerical solution of Massuchetto et al. [4] was obtained using the Aspen HYSYS® software, while the current numerical code was developed using MATLAB and REFPROP software.

The exergy destruction values for various components of the

**Table 3. The design variables and their ranges for CCRS optimization**

| Decision variable | Range of variation |
|---|---|
| Binary Refrigerant Mixtures for LTC ($R_{LTC,f}$, $R_{LTC,s}$) | [$CO_2$, DME, Propylene] |
| The mass fraction of the first refrigerant in LTC | $0 < Mf_{LTC} < 1$ |
| Binary Refrigerant Mixtures for HTC ($R_{HTC,f}$, $R_{HTC,s}$) | [$CO_2$, DME, Propylene] |
| The first refrigerant mass fraction at HTC | $0 < Mf_{HTC} < 1$ |
| The saturated vapor temperature at the condenser inlet | $40 \le T_{6,sv} \le 80$ °C |
| The saturated vapor temperature at the CHX inlet | $-5 \le T_{2,sv} \le 40$ °C |
| The evaporator inlet temperature | $-40 \le T_4 \le -21$ °C |
| The two-phase temperature at the CHX inlet | $-10 \le T_8 \le 10$ °C |

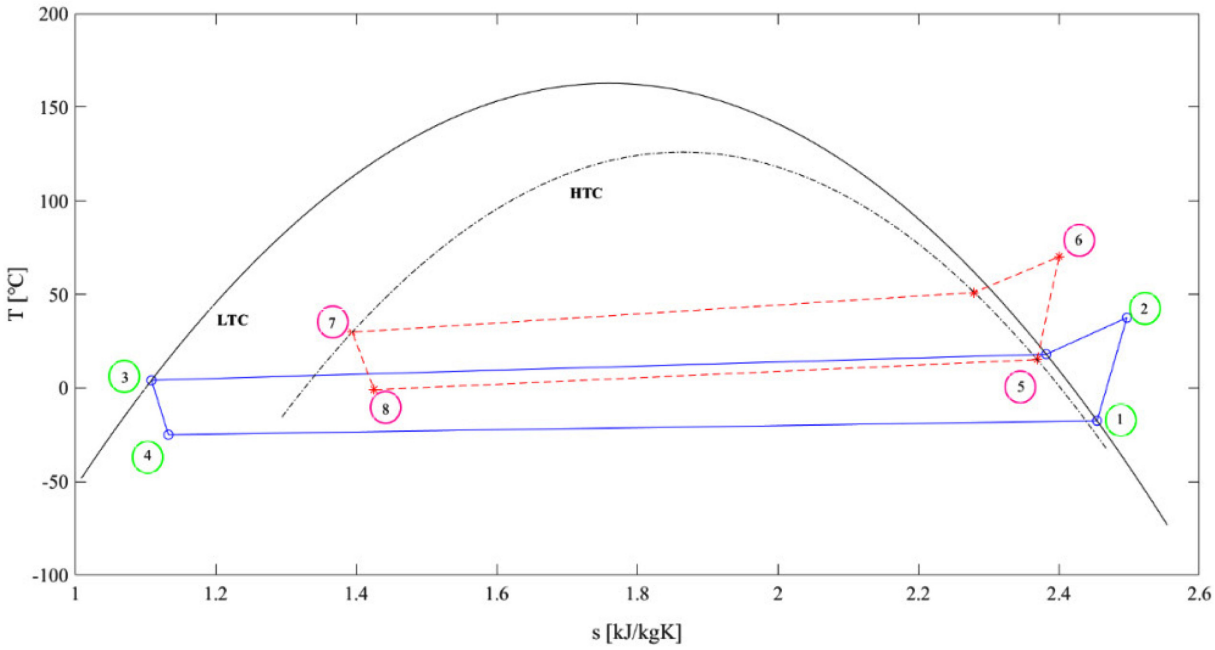


**Figure 2. The T-s diagram of the mixed refrigerant used in CCRS.**

**Table 4. Verification of numerical code**

| Inputs | | | | | | | |
|---|---|---|---|---|---|---|---|
| Mixed Refrigerant | | | | | R744/RE170 | | R744/R1270 |
| $CO_2$ (wt%) | | | | | HTC<br>LTC | | 20<br>10 | | 30<br>10 |
| $T_{cond,sv}$ (°C) | | | | | HTC ($T_{6,sv}$)<br>LTC ($T_{2,sv}$) | | 53<br>25 | | 51<br>18 |
| $T_{evp,in}$ (°C) | | | | | HTC ($T_8$)<br>LTC ($T_4$) | | 6<br>-25 | | -1<br>-25 |
| Outputs | | | | | | | |
| | | [4] | Numerical code | Relative error (%) | [4] | Numerical code | Relative error (%) |
| $T_{comp,out}$ (°C) | HTC ($T_6$) | 71 | 69 | -2.8 | 75 | 70.07 | -6.57 |
| | LTC ($T_2$) | 56 | 54.65 | -2.4 | 39 | 37.55 | -3.7 |
| $P_{cond}$ (kPa) | HTC | 1555 | 1540.5 | -0.93 | 3115 | 3040.4 | -2.39 |
| | LTC | 651 | 654.9 | 0.6 | 1061 | 1070.7 | 0.9 |
| $\dot{m}$ (kg. $s^{-1}$) | HTC | 0.35 | 0.3453 | -1.34 | 0.47 | 0.45 | -4.25 |
| | LTC | 0.26 | 0.2634 | 1.31 | 0.29 | 0.299 | 3.1 |
| $\dot{W}_t$ (kW) | | 42.7 | 41.745 | -2.24 | 46 | 43.45 | -5.54 |
| COP | | 2.34 | 2.395 | 2.35 | 2.17 | 2.3 | 6 |
| η (%) | | 34 | 35.18 | 3.47 | 31 | 33.69 | 8.68 |

CCRS (for $CO_2$/Propylene pairs) were depicted in Fig. 3. Additionally, the effect of each piece of equipment on total exergy destruction ($\delta_i$) was presented as a pie chart in Fig. 4. The results were presented for $CO_2$/Propylene mixtures on LTC and HTC with $CO_2$ weight percentages listed in Table 4.

As shown in Figs. 3 and 4, the condenser has the highest exergy destruction value (30%). This was due to the high temperature difference between the refrigerant and the environment in the condenser. Additionally, the LTC expansion valve showed the lowest exergy destruction value (7%) because of its lower entropy increase compared to the HTC expansion valve. The required compressor power for the LTC and HTC systems was 19.49 kW and 23.96 kW, respectively. Using the economic and operational parameters presented in Table 5, the total capital and maintenance cost rates for the base case were 6.84 $/hr, while the operational cost rate was 3.04 $/hr. Therefore, the total cost rate for this situation was 9.88 $/hr.

Using an initial population of 50 and a maximum of 150 iterations, a multi-objective optimization was performed. The NSGA-II crossover and mutation rates were set at 70% and 30%, respectively. The optimization was conducted for the design variables presented in Table 3, with a constant cooling capacity of 100 kW. The results of the optimization were shown in Fig. 5, which illustrated the best

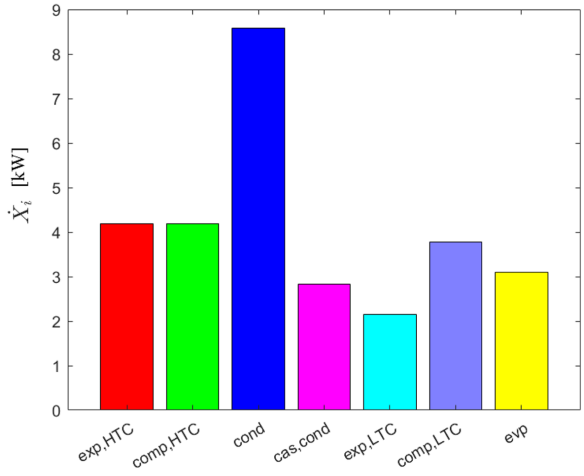


**Fig. 3. Exergy destruction across various components of CCRS.**

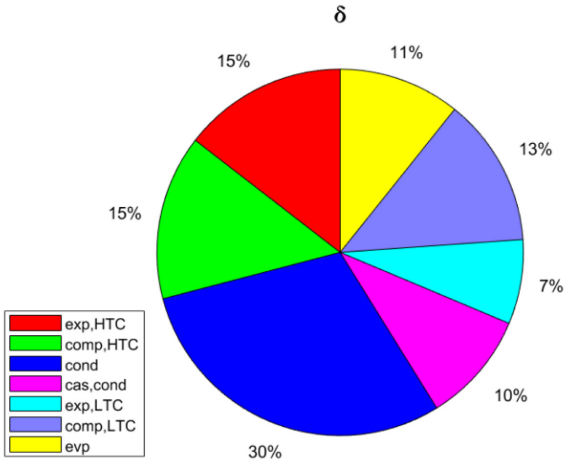


**Fig. 4. Contribution of CCRS components to total exergy destruction ($\delta_i$ values).**

**Table 5. The economic and operational parameters for CCRS**

| | |
|---|---|
| Operating period ($n$) | 15 years |
| Interest rate ($i$) | 40% |
| Operational hours of the system in a year ($N$) | 6570 hr |
| Maintenance factor (φ) | 1.06 |
| Electricity cost ($C_{el}$) | 0.07 $/kWh |

solution outputs for the three objective functions.

Fig. 5 showed that there were only four solutions that represented the best non-dominated results for increasing the COP and $\eta$ while decreasing the total cost rate ($\dot{C}_t$). Additional details about the optimized best solutions were provided in Table 6.

As shown in Table 6, the best refrigerant for the low temperature cycle of CCRS was a mixture of DME and propylene, with approximate mass fractions of 0.33 and 0.67, respectively. In contrast, the best refrigerant for the high temperature cycle of CCRS was a mixture of $CO_2$ and DME, with approximate mass fractions of 0.16 and 0.84, respectively. Regarding economic factors, the total cost rates ($\dot{C}_t$) for all optimization results (Nos. 1 to 4) were significantly lower than the best optimization result reported by Massuchetto et al. [4] (9.88 $/hr).

The best solution with the highest COP and exergy efficiency ($\eta$) and with a slightly higher total cost rate (No.2) was selected to compare the three-objective optimization results with the base data. By comparing the optimization best solution (No.2) with the best optimization results reported in the literature (Table 4), the COP and exergy efficiency ($\eta$) can be improved by about 15.55% and 17.74%, respectively. Also, the total cost rate of CCRS decreased from 9.88 $/hr to 9.28 $/hr (approximately 6.07% reduction). For the best solution, the overall capital and maintenance cost rates was 6.75 $/hr, while the operational cost rate was 2.53 $/hr, showing reductions of 1.32% and 16.78%

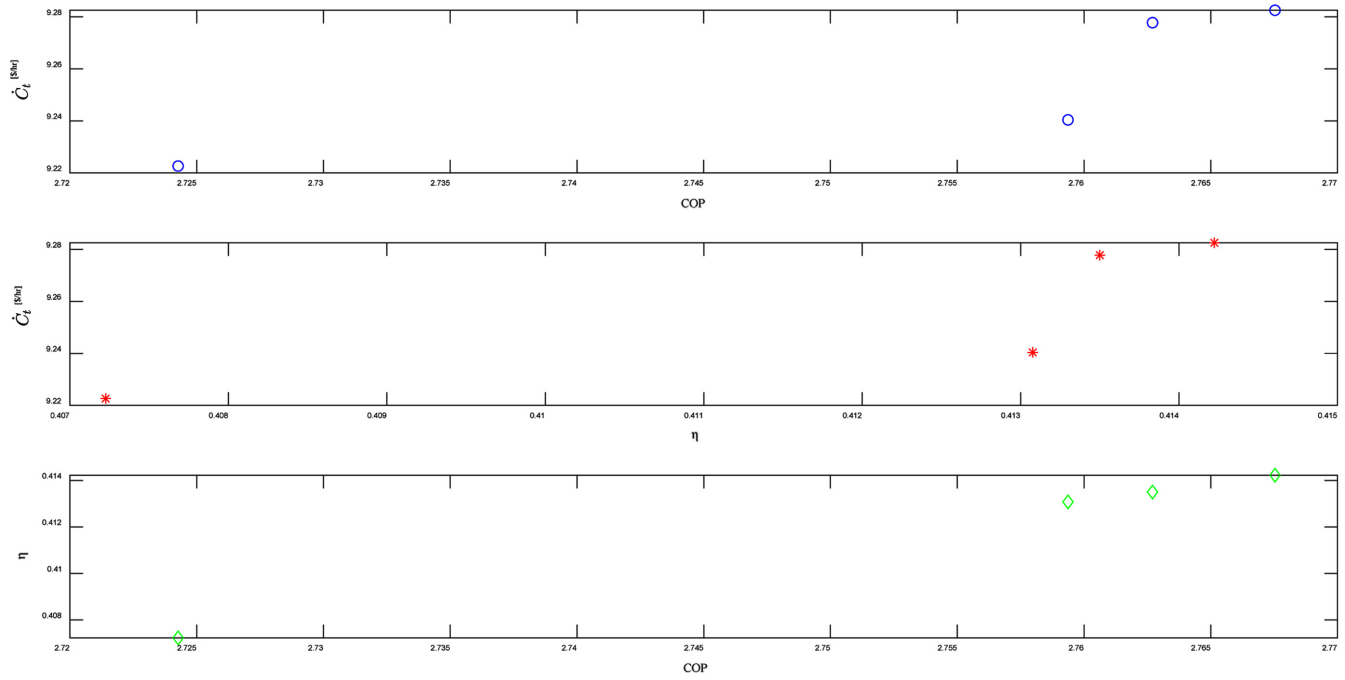


**Fig. 5. Three objective optimization outputs.**

**Table 6. The best non-dominated results for three-objective optimization of CCRS**

| Best Solutions | No.1 | No.2 | No.3 | No.4 |
|---|---|---|---|---|
| Binary Refrigerant Mixtures for LTC | | [DME, Propylene] | | |
| $Mf_{LTC}$ | 0.3536 | 0.3283 | 0.3373 | 0.3283 |
| Binary Refrigerant Mixtures for HTC | | [$CO_2$, DME] | | |
| $Mf_{HTC}$ | 0.1529 | 0.1596 | 0.1556 | 0.1596 |
| $40 \le T_{6,sv} \le 80$ °C | 47.2632 | 46.5053 | 46.7212 | 46.5822 |
| $-5 \le T_{2,sv} \le 40$ °C | 13.2252 | 14.0450 | 13.7997 | 14.0450 |
| $-40 \le T_4 \le -21$ °C | −24.0185 | −23.9769 | −23.8658 | −23.9769 |
| $-10 \le T_8 \le 10$ °C | 4.4147 | 4.7356 | 4.7384 | 4.7356 |
| COP | 2.7243 | 2.7675 | 2.7594 | 2.7627 |
| η (%) | 40.72 | 41.42 | 41.31 | 41.35 |
| $\dot{C}_t$ [$/hr] | 9.223 | 9.283 | 9.240 | 9.278 |

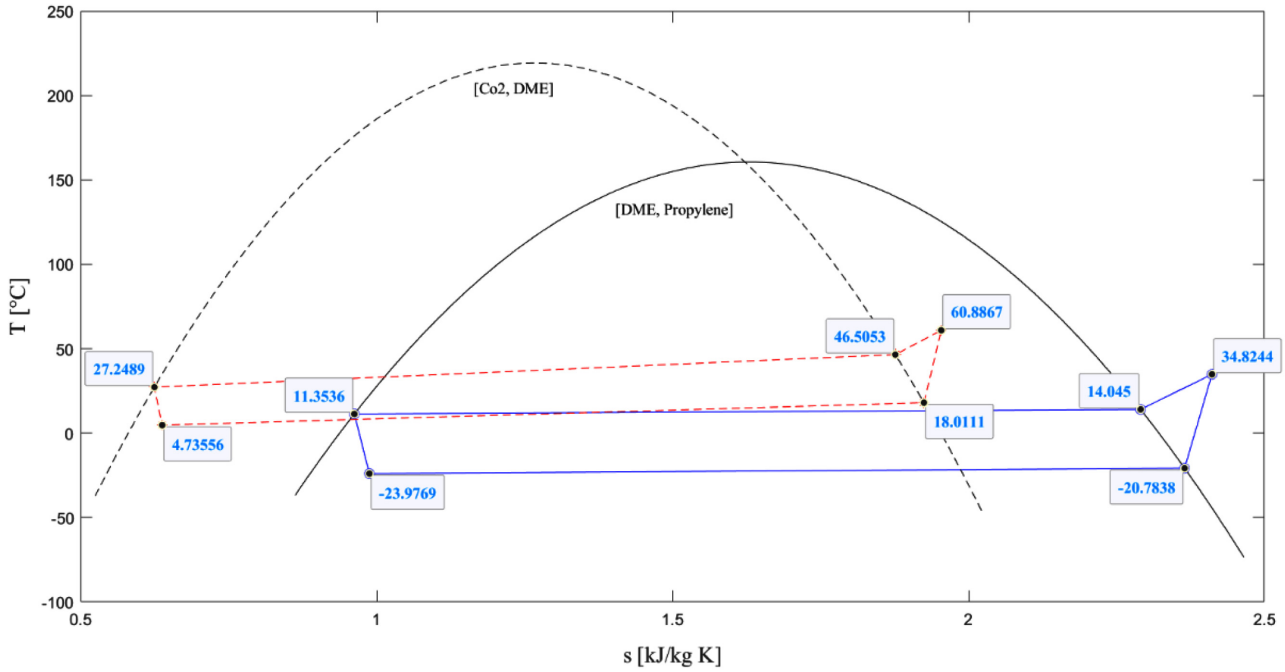


**Fig. 6. The T-s diagram for the optimized solution (No.2).**

compared to the base case, respectively. The results indicated that using multi-objective optimization can led to significant savings in operational costs, while its effect on initial and maintenance costs was negligible.

The T-s diagram for the selected optimization solution (No.2) was presented in Fig. 6. This figure differed slightly from the base T-s diagram shown in Fig. 2, as it used the binary mixtures of {DME and propylene} and {$CO_2$ and DME} for the low temperature cycle and high temperature cycle of the CCRS. It was important to note that the temperature data for all points in the cycle were depicted in this figure. Additionally, the temperature glide during phase changes in the condenser, evaporator, and cascade heat exchanger was visible.

The exergy destruction values for various components of the CCRS for the selected optimization best solution (No.2) were depicted in Fig. 7. Additionally, the effect of each component on total exergy destruction ($\delta_i$) for this case was presented as a pie chart in Fig. 8.

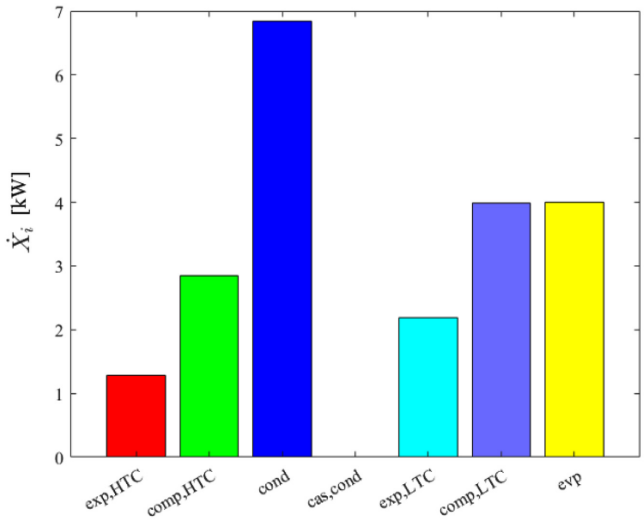


**Fig. 7. Exergy destruction for various components of CCRS (optimization result No.2).**

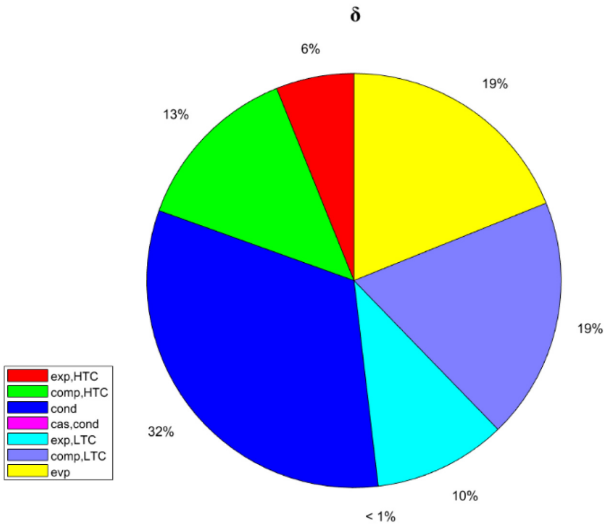


**Fig. 8. The $\delta_i$ values for various components of CCRS (optimization result No.2).**

As shown in Figs. 7 and 8, the highest and lowest exergy destruction values can be attributed to the condenser and cascade heat exchanger (CHX), respectively. The exergy destruction of the cascade condenser was very small, making its effect on total exergy destruction negligible (less than 1%). Overall, the three-objective optimization of CCRS can decrease the total exergy destruction of the cascade cycle from 28.81 kW to 21.17 kW, which was equivalent to a 26.5% reduction.

Finally, the LTC and HTC required compressor powers for the optimized solution were 20.34 kW and 15.79 kW, respectively. The comparison of compressors work between the base case and the optimized solution (No.2) showed a slight increase of about 4.36% for the LTC compressor power consumption and a significant reduction of 34.01% for HTC compressor required work. Also, the total work for the optimized solution demonstrated a 16.85% reduction. Moreover, the mixed refrigerant temperature leaving the HTC compressor decreased from 70.07℃ to 60.89℃, which can lead to lower depreciation and better performance.

## 4. Conclusion

This study presented a method for three-objective optimization of a compression cascade refrigeration system (CCRS) using mixed refrigerants. The method addressed energy, exergy, and economic aspects of the CCRS. The optimization process focused on maximizing the cycle's coefficient of performance (COP) and exergy efficiency ($\eta$), while minimizing the total annual cost rate ($\dot{C}_t$), which included initial, maintenance, and electricity costs over the system's lifetime. Using the NSGA-II algorithm, ten design variables were employed. These include two refrigerants (from $CO_2$, DME, and propylene) and their mass fractions for the low-temperature (LTC) and high-temperature (HTC) cycles, along with four temperatures. The remaining design variables were the saturated vapor temperatures in the condenser and cascade condenser inlets ($T_{8,sv}$, $T_{2,sv}$) and the refrigerant temperatures in the evaporator and heat exchanger inlets ($T_4$, $T_8$). Constraints included cooling capacity and cooling water temperatures for the condenser and evaporator. With a constant cooling capacity of 100 kW, the best refrigerant mixtures for the LTC and HTC were found to be {DME and propylene} and {$CO_2$ and DME}, with optimal mass fractions around 0.33 for DME in LTC and 0.16 for $CO_2$ in HTC. The optimized results showed a moderate increase in COP and $\eta$, alongside a slight decrease in $\dot{C}_t$. Notably, the selected optimization result indicated an increase in COP from 2.3 to 2.7675 and $\eta$ from 33.69% to 41.42%, while reducing $\dot{C}_t$ from 9.88 to 9.28 \$/hr. The highest exergy destruction was attributed to the condenser, while the LTC expansion valve and cascade condenser showed the lowest destruction levels. In the optimized solution, the exergy destruction of the cascade condenser was minimal and had negligible impact on the overall exergy analysis. Overall, the proposed multi-objective optimization resulted in significant operational cost savings, with minimal effects on initial and maintenance costs. Finally, the underlying framework can be adapted to accommodate a larger number of refrigerant candidates, and HTC compressor discharge temperature. This can be achieved by incorporating additional design variables, and should be considered in the future works.

## Nomenclature

| | |
|---|---|
| $A$ | : Heat exchanger area [$m^2$] |
| $CCRS$ | : Compression cascade refrigeration system |
| $CHX$ | : Cascade heat exchanger |
| $COP$ | : Coefficient of performance |
| $CRF$ | : Capital recovery factor |
| $CRS$ | : cascade refrigeration system |
| $C_{el}$ | : Electricity cost [\$/kWh] |
| $\dot{C}$ | : Cost rate [\$/hr] |
| $\dot{C}_{op}$ | : Operational cost rate [\$/hr] |
| $DME$ | : Dimethyl Ether |
| $h$ | : Enthalpy [kJ/kg] |
| $HTC$ | : High-temperature cycle |
| $i$ | : Interest rate |
| $LTC$ | : Low-temperature cycle |
| $\dot{m}$ | : Mass flow rate [kg/s] |
| $Mf$ | : Mass fraction of 1$^{st}$ refrigerant |
| $n$ | : System lifetime [year] |
| $N$ | : Annual operational hours of the system [hr] |
| $NBP$ | : Normal Boiling Point |
| $P$ | : Pressure [kPa] |
| $\dot{Q}$ | : Heat transfer rate [kW] |
| $R$ | : Refrigerant |
| $s$ | : Entropy [kJ/kg K] |
| $T$ | : Temperature [$^o$C or K] |
| $VCRS$ | : Vapor compression refrigeration system |
| $\dot{X}$ | : Exergy destruction [kW] |

$Z$ : Capital cost [$]
$\dot{Z}$ : Capital and maintenance cost rates [$/hr]

**Subscripts**

0 : Ambient
1 : Saturated refrigerant leaving evaporator
2 : Refrigerant leaving LTC compressor
3 : Condensed refrigerant leaving CHX
4 : Refrigerant temperature in the evaporator inlet
5 : Evaporated refrigerant leaving CHX
6 : Refrigerant leaving HTC compressor
7 : Condensed refrigerant leaving condenser
8 : Refrigerant temperature in the CHX inlet (after HTC expansion valve)
cas : Cascade
CL : Cold refrigerated space
cond : Condenser
evp : Evaporator
exp : Expansion valve
HS : Heat Source
HTC, f : High-temperature cycle, first
HTC, s : High-temperature cycle, second
in : Inlet
LTC, f : Low-temperature cycle, first
LTC, s : Low-temperature cycle, second
out : Outlet
sl : Saturated liquid
sv : Saturated vapor
Surr : Surrounding
t : Total

**Greek Symbols**

$\delta$ : Contribution on total exergy destruction
$\eta$ : Exergy efficiency
$\varphi$ : Maintenance factor
$\psi$ : Flow physical exergy [kJ/kg]

## References


1. Fernández-Seara, J., Sieres, J. and Vázquez, M., "Compression–Absorption Cascade Refrigeration System," *Appl. Therm. Eng.*, **26**(5), 502-512(2006).
2. Alberto Dopazo, J., Fernández-Seara, J., Sieres, J. and Uhía, F. J., "Theoretical Analysis of a $CO_2$–$NH_3$ Cascade Refrigeration System for Cooling Applications at Low Temperatures," *Appl. Therm. Eng.*, **29**(8), 1577-1583(2009).
3. Di Nicola, G., Polonara, F., Stryjek, R. and Arteconi, A., "Performance of Cascade Cycles Working with Blends of $CO_2$ + Natural Refrigerants," *IJR*, **34**(6), 1436-1445(2011).
4. Massuchetto, L. H. P. R., Nascimento, B. C. d., Carvalho, S. M. R. d., Araújo, H. V. d. and d'Angelo, J. V. H., "Thermodynamic Performance Evaluation of a Cascade Refrigeration System With Mixed Refrigerants: R744/R1270, R744/R717 and R744/RE170," *IJR*, **106**, 201-212(2019).
5. Sánchez, D., Vidan-Falomir, F., Nebot-Andrés, L., Llopis, R. and Cabello, R., "Alternative Blends of $CO_2$ for Transcritical Refrigeration Systems. Experimental Approach and Energy Analysis," *Energy Convers. Manage.*, **279**, 116690(2023).
6. Sun, Z., Liang, Y., Liu, S., Ji, W., Zang, R., Liang, R., and Guo, Z., "Comparative Analysis of Thermodynamic Performance of a Cascade Refrigeration System for Refrigerant Couples R41/R404A and R23/R404A," *Appl. Energy*, **184**, 19-25(2016).
7. Nasruddin, Sholahudin, S., Giannetti, N. and Arnas, "Optimization of a Cascade Refrigeration System Using Refrigerant $C_3H_8$ in High Temperature Circuits (HTC) and a Mixture of $C_2H_6$/$CO_2$ in Low Temperature Circuits (LTC)," *Appl. Therm. Eng.*, **104**, 96-103(2016).
8. Patel, V., Panchal, D., Prajapati, A., Mudgal, A. and Davies, P., "An Efficient Optimization and Comparative Analysis of Cascade Refrigeration System Using $NH_3$/$CO_2$ and $C_3H_8$/$CO_2$ Refrigerant Pairs," *IJR*, **102**, 62-76(2019).
9. Golbaten Mofrad, K., Zandi, S., Salehi, G. and Khoshgoftar Manesh, M. H., "4E Analyses and Multi-objective Optimization of Cascade Refrigeration Cycles with Heat Recovery System," *TSEP*, **19**, 100-115(2020).
10. Jain, V., Rawat, R., Sachdeva, G. and Kumar, V., "Multi-Objective Optimization of Cascade Refrigeration System Using the Concept of Modified and Advanced Exergy, Risk Level and Thermal Inventory," *Int. J. Air-Cond. Refrig*, **28**(4), 205-236(2020).
11. Zhu, Y. D., Peng, Z. R., Wang, G. B. and Zhang, X. R., "Thermodynamic Analysis of a Novel Multi-target-temperature Cascade Cycle for Refrigeration," *Energy Convers. Manage.*, **243**, 114-138(2021).
12. Yoon, J. H., Yoon, J. I., Son, C. H. and Seol, S. H., "Energy and Exergy Analysis of Cascade Mixed Refrigerant Joule & Ndash; Thomson System with the Application of a Precooler," *Energies*, **16**(19), 69-91(2023).
13. Ghosh, A., Sharma, A., Varshney, B., Chirag, and Kashyap, P. K., "A Theoretical Thermodynamic Analysis of R1234yf/$CO_2$ Cascade Refrigeration System," *Recent Advances in Manufacturing and Thermal Engineering*, Mar., Singapore(2022).
14. Liu, J., Gao, Y., Lu, C. and Ahmad, M., "Enhancing Energy and Exergy Performance of a Cascaded Refrigeration Cycle: Optimization and Comparative Analysis," *J. Clean. Prod.*, **438**, 140-167 (2024).
15. Liu, Z., Ji, S., Tan, H. Yang, D. and Cao, Z., "An Ultralow-temperature Cascade Refrigeration Unit With Natural Refrigerant Pair R290-R170: Performance Evaluation Under Different Ambient and Freezing Temperatures," *TSEP*, **46**, 102-122(2023).
16. Ye, W., Liu, F., Yan, Y. and Liu, Y., "Application of Response Surface Methodology and Desirability Approach to Optimize the Performance of An Ultra-low Temperature Cascade Refrigeration System," *Appl. Therm. Eng.*, **239**, 122-130(2024).
17. Rezayan, O. and Behbahaninia, A., "Thermoeconomic Optimization and Exergy Analysis of $CO_2$/$NH_3$ Cascade Refrigeration Systems," *Energy*, **36**(2), 888-895(2011).
18. Heggs, P. J., "Minimum Temperature Difference Approach Concept in Heat Exchanger Networks," *Heat Recovery Systems and CHP*, **9**(4), 367-375(1989).

19. Oh, J. S., Binns, M., Park, S. and Kim, J. K., "Improving the Energy Efficiency of Industrial Refrigeration Systems," *Energy*, **112**, 826-835(2016).
20. McLinden, M. O. and Radermacher, R., "Methods for Comparing the Performance of Pure and Mixed Refrigerants in the Vapour Compression Cycle," *IJR*, **10**(6), 318-325(1987).
21. Aminyavari, M., Najafi, B., Shirazi, A. and Rinaldi, F., "Exergetic, Economic and Environmental (3E) Analyses, and Multi-objective Optimization of a $CO_2/NH_3$ Cascade Refrigeration System," *Appl. Therm. Eng*., **65**(1), 42-50(2014).
22. Bejan, A., Tsatsaronis, G. and Moran, M. J., *Thermal design and optimization*, John Wiley & Sons, (1995).
23. Konak, A. D., Coit, W. and Smith, A. E., "Multi-objective Optimization Using Genetic Algorithms: A Tutorial," *Reliab. Eng. Syst. Saf*., **91**(9), 992-1007(2006).

**Authors**

**Mostafa Dehghani:** Assistant Professor, Department of Engineering, Meybod university, Yazd, Iran, HYPERLINK; mailto:m_dehghani@meybod.ac.ir, m_dehghani@meybod.ac.ir; Department of Mechanical Engineering, University of Sistan and Baluchestan, Zahedan, Iran, HYPERLINK; mailto:m_dehghani@eng.usb.ac.ir, m_dehghani@eng.usb.ac.ir

**Mohsen Mozafari_Shamsi:** Assistant Professor, Department of Engineering, Meybod university, Yazd, Iran, HYPERLINK; mailto:mozafari@meybod.ac.ir, mozafari@meybod.ac.ir